9. C. C. Mei, "Collapse of a homogeneous fluid mass in a stratified fluid," in: Proceedings of the Twelfth International Congress on Applied Mechanics, Stanford University (1968).
10. V. I. Nikishov and A. G. Stetsenko, "Formation of internal waves generated by the collapse of a homogeneous 'spot' in a stratified liquid," in: Hydromechanics [in Russian], No. 32, Naukova Dumka, Kiev (1975).

INTERACTION BETWEEN TURBULENT BOUNDARY LAYERS IN A RIGHT DIHEDRAL CORNER

V. I. Kornilov and A. M. Kharitonov

UDC 532.526.4

The interaction between two adjacent turbulent boundary layers which occurs in longitudinal flow over intersecting surfaces pertains to complex forms of viscous flow. Such flow is very often encountered in practice, for instance, at the joints between individual parts of aircraft, in flow around cross-shaped and V-shaped wings, etc. However, in spite of its practical importance, the nature of viscous interaction in corner configurations has not yet been investigated experimentally to a sufficient extent. As a rule, no allowance is made for the three-dimensional nature of corner flow in theoretical investigations, and, therefore, the results are in poor agreement with experimental data.

The present article is concerned with an experimental investigation of the integral characteristics of the boundary layer, determination of the extent of the interaction zone for different Reynolds numbers, and a study of the effect of the longitudinal pressure gradient.

The experiments are performed in the low-turbulence T-324 aerodynamic tunnel at the Institute of Theoretical and Applied Mechanics, Siberian Branch, Academy of Sciences of the USSR [1], using a right dihedral simulator (Fig. 1). Take-off openings, 3, with a diameter of 0.5 mm are provided on both sides 1 for measuring the static pressure. Both the fore and aft parts of the dihedral sides have a semielliptical shape with a 1:12 ratio of the semiaxes. The static pressure along the length of the simulator is varied by means of two rear-end flaps, 2. A clear-plastic dummy wall, 4, is mounted in the working section of the aerodynamic tunnel in order to ensure the assigned longitudinal pressure gradient at the surface of the simulator. The pressure gradient varies according to the degree to which the operating section is blocked, while the gradient sign is determined by the shape of the contour of the operating section artifically created by the dummy wall. Both positive and negative static pressure gradients $d\bar{p}/dx$ ($\bar{p} = (p - p_\infty)/q_\infty$ is the pressure coefficient) can thereby be created at the simulator surface.

The experiments are performed at unperturbed flow velocities from 10 to 52 m/sec, which corresponds to individual Reynolds numbers $Re_1 = (0.7-3.2) \cdot 10^6$ m^{-1}. A well-developed turbulent boundary layer is produced by means of a turbulence generator consisting of coarse-grained emery paper 10 mm wide, which is pasted on along the spread of the corner at a distance of 10 mm from the leading edge.

The total and the static pressures and the direction of the velocity vector in the boundary layer are measured by means of miniature pneumatic tubes, 5, the geometric characteristics of which are shown in Fig. 1. Special calibration checks have shown that, with an accuracy to 1%, the flat and the cylindrical tubes are not sensitive to downwashes to up to 9° and 22°, respectively. Similar calibrations have also been performed in the investigated velocity range for a double-barrelled pneumatic tube, which is used for determining the direction of the velocity vector in the boundary layer of the dihedral corner. The thus obtained data on the downwash angles in two mutually perpendicular planes and the knowledge of the longitudinal velocity component make it possible to determine the transverse velocity component.

In order to verify the hypothesis concerning the constancy of static pressure across the boundary layer, we measured the static pressure profiles by means of a special microtube, which was also calibrated beforehand. The results of these experiments have shown that the maximum change in static pressure along the height of the boundary layer occurs in the bisecting plane and is equal to $\pm 0.007 q_\infty$. Allowance for this degree

Novosibirsk. Translated from Zhurnal Prikladnoi Mekhaniki i Tekhnicheskoi Fiziki, No. 3, pp. 69-76, May-June, 1978. Original article submitted July 7, 1977.

0021-8944/78/1903-0336 $07.50

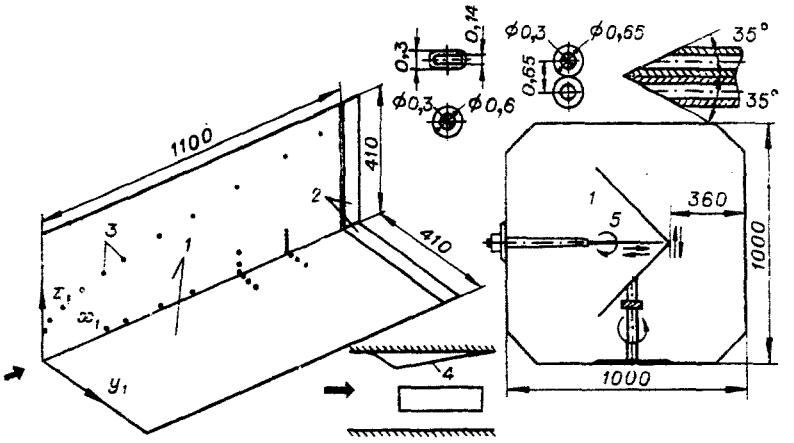

Fig. 1

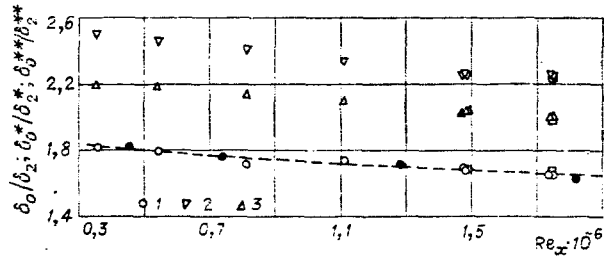

Fig. 2

of static pressure instability alters the integral characteristics of the boundary layer by less than 0.7%. Therefore, the static pressure variation was neglected.

Estimates based on data from many experiments indicate that the relative random errors in measuring the characteristics δ^* and δ^{**}, calculated with respect to the longitudinal velocity component in the boundary layer, do not exceed 0.2%. Neglect of the transverse component may produce an additional error of approximately 0.5%.

Figure 2 (points 1-3, respectively) provides the relative values of the boundary-layer thickness δ_0/δ_2, the displacement thickness δ_0^*/δ_2^*, and the momentum loss thickness $\delta_0^{**}/\delta_2^{**}$ (the subscript 0 pertains to the boundary-layer characteristics in the bisecting plane of the dihedral corner $y_1 = z_1 = 0$, while the subscript 2 pertains to the characteristics at a distance from this plane where viscous interaction vanishes) as functions of the Re_x number, calculated with respect to the unperturbed flow parameters and the effective distance x from the beginning of the turbulent boundary layer. The data given for $Re_x \simeq 1.72 \cdot 10^6$ have been obtained by means of both a pneumatic tube and a 55D00 cooling-power anemometer, manufactured by the DISA company. The deviations of these values fall within the limits of experimental error. In the region where viscous interaction is absent, the experimental data are in good agreement with the results of numerical calculations, performed according to the method described in [2]. For instance, the mean deviation of δ_2^{**}, calculated by means of the expression

$$\frac{\Delta\delta_2^{**}}{\delta_{\text{theor}}^{**}} = \frac{\delta_{2\,\text{exp}}^{**} - \delta_{2\,\text{theor}}^{**}}{\delta_{2\,\text{theor}}^{**}} \cdot 100\ \%,$$

does not exceed 2.4%.

Figure 2 also provides the experimental data on δ_0/δ_2, obtained in [3] (solid circles). The results obtained in different experiments are in satisfactory mutual agreement; they can be approximated with a sufficient degree of accuracy by the expression (dashed curve in Fig. 2)

$$\delta_0/\delta_2 = C(\text{Re}_x)^{-n},$$

where C = 5.15 and n = 0.08 are empirical constants.

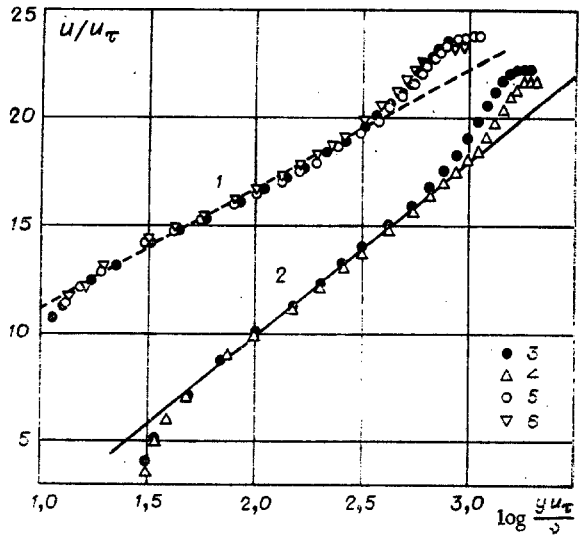

Fig. 3

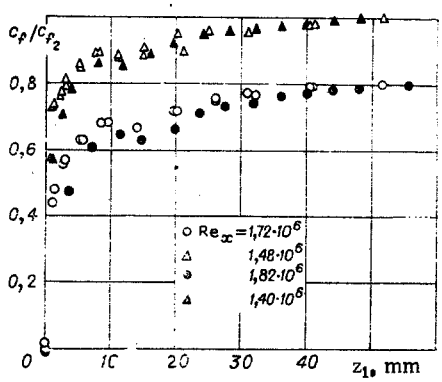

Fig. 4

Considering the above dependences, we see that, in the investigated range of Re_x numbers, the integral characteristics of the boundary layer in the bisecting plane of the coupled surfaces exceed by a factor of 1.6-2.5 the corresponding values outside the interaction region. The latter values, however, increase at a higher rate along the simulator length. This is why a slight reduction in the relative values δ_0/δ_2, δ_0^*/δ_2^*, and $\delta_0^{**}/\delta_2^{**}$ is observed with an increase in the Reynolds number.

Figure 3 shows, for $d\bar{p}/dx = 0$, several experimental velocity profiles, measured outside the zone of interaction between the boundary layers (the upper group of points) and plotted in the form of the wall law:

$$\varphi = f(\lg \eta),$$

where $\varphi = u/u_\tau$; $\eta = (y_1 u_\tau)/\nu$; $u_\tau = \sqrt{\tau_w/\rho} = u_\delta \sqrt{c_f/2}$. For determining the local values of the friction coefficient c_f, the integral momentum relationship for a flat plate $c_f/2 = d\delta^{**}/dx$ is used in this case; the derivative $d\delta^{**}/dx$ is determined graphically with respect to the theoretical curves that average the experimental values of $\delta_2^{**}(x)$. The dimensionless velocity profiles expressed in terms of the adopted variables have linear sections, and, even for $z_1 \approx 3\delta_2$, they are in satisfactory agreement with the well-known relationship $u/u_\tau = A \log (yu_\tau/\nu) + B$, which holds for a flat plate in incompressible flow [curve 1 in Fig. 3; $z_1 \simeq 60$ mm; 3-6) x = 890; 700; 540; 350 mm, respectively].

It should be noted that, if the variable dynamic velocity $u_\tau(z_1)$ in the vicinity of the corner line is used as the scale value, the velocity distribution in the bisecting plane (the lower group of points) can also be approximated with satisfactory accuracy by a similar dependence, using, however, different values of the coefficients A and B (A = 8.12; B = −1.38, curve 2 in Fig. 3; $y_1 = z_1 = 0$). It is impossible to use the integral momentum relationship for determining the value of c_f because of the three-dimensional nature of the flow in the interaction zone. At the same time, a preliminary estimate of the experimental values of c_f outside the interaction zone, based on the velocity gradient near the wall, has shown satisfactory agreement with the results obtained from the integral momentum relationship and by numerical calculations based on the method described in [2].

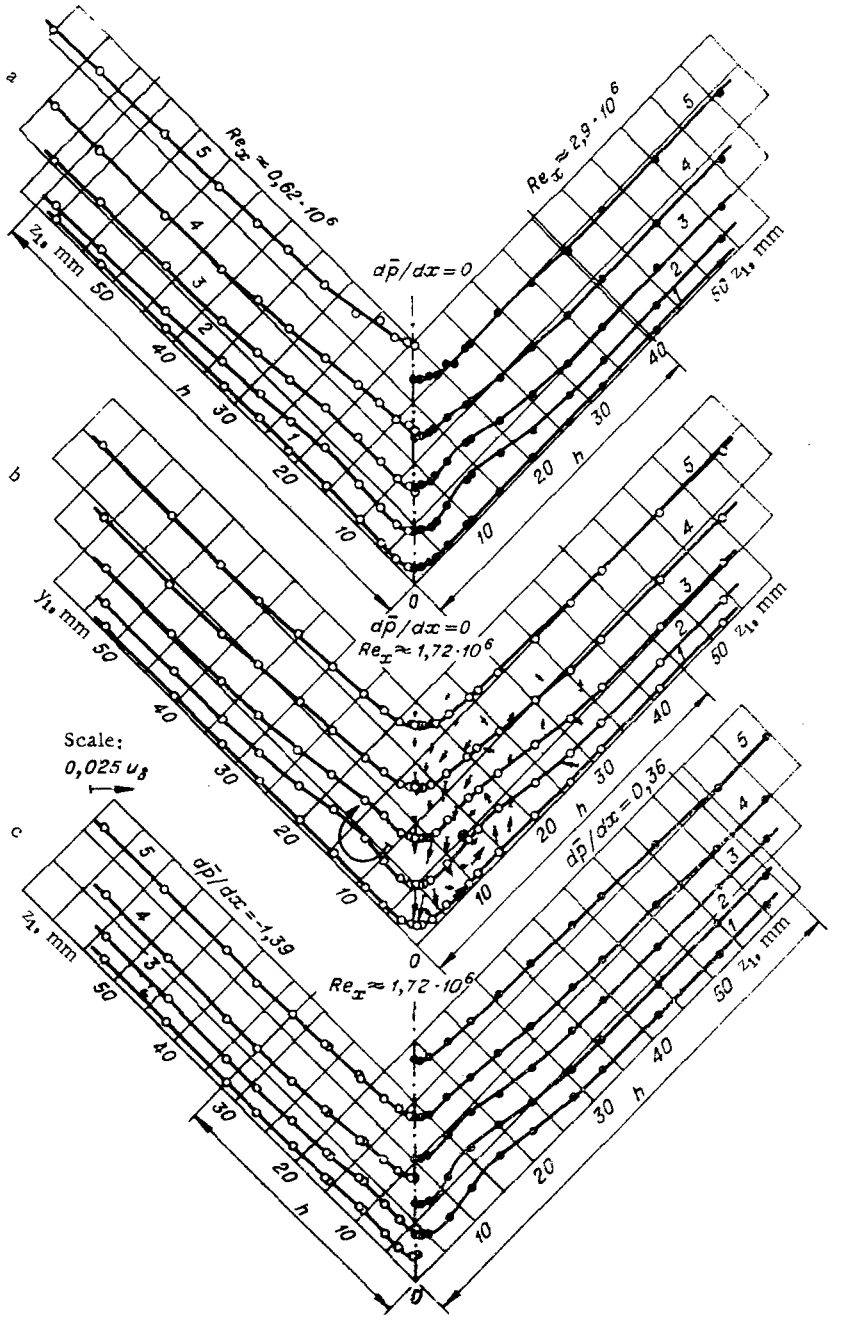

Fig. 5

A similar approach to the determination of the friction coefficient is also used for the interaction region. These data for two transverse cross sections of the simulator are given in Fig. 4 for $d\bar{p}/dx = 0$ in the form of the relationship $c_f/c_{f_2} = f(z_1)$ (open circles). For comparison, there are also shown the results from [3], where the value of c_f was measured directly by means of Preston sensors (solid circles). Allowing for certain differences in the experimental conditions, it can be said that these data are in satisfactory mutual agreement. It is evident that, in approaching the line of intersection between the surfaces ($y_1 = z_1 = 0$), the local friction coefficient gradually diminishes from the value of c_{f_2} on a flat plate to a value approaching zero in the bisecting plane. It is noteworthy that there is a local minimum of the relationship $c_f/c_{f_2}(z_1)$ located at a distance of ~12-15 mm from the intersection between the surfaces, which corresponds to $z_1 \simeq (0.8\text{-}1.0)\delta_2$. It can be assumed that this is connected with vortex flow in the vicinity of the bisecting plane, the extent of which in the transverse cross section increases with distance from the leading edge.

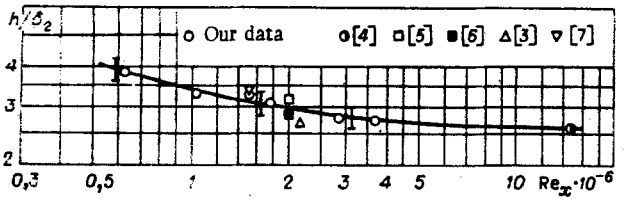

Fig. 6

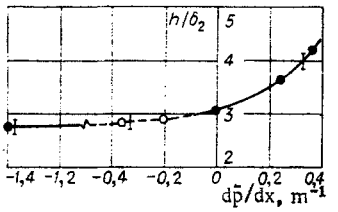

Fig. 7

Thus, the velocity distribution in the bisecting plane and its neighborhood has a character different from that on a flat plate under similar conditions. Transition from one flow form to another occurs smoothly within the defined zone, which is commonly referred to as the region of interaction between boundary layers. The extent of this region in the transverse direction h can be determined with respect to the velocity distribution in the transverse section of the corner. A typical distribution of isotachs for x = 890 mm is shown in Fig. 5, where curve 1 corresponds to the velocity ratio $u/u_\delta = 0.60$; the other curves pertain to the following values of this ratio: 2) 0.70; 3) 0.80; 4) 0.90; 5) 0.99. One notices that there are two regions, in one of which the isotachs are parallel to the side of the corner, while they are considerably distorted in the other. The distortion of isotach contours is due to the presence of a secondary flow. In order to investigate this flow, we have performed detailed measurements of the velocity profiles for the transverse flow in the bisecting plane as well as at various distances from it. The intensities and directions of this flow are indicated by arrows against the background field of the longitudinal velocity component (Fig. 5b). The pattern revealed is in agreement with experimental data from [3]. It is evident that, as a result of interaction between turbulent boundary layers, the transverse flow moves along the bisecting plane toward the corner line, and from this line further along the corner side, thereby forming a circulation flow. The maximum velocity of the transverse flow is equal to $0.025u_\delta$, which is reached in the bisecting plane at a distance of approximately 40% of the boundary-layer thickness.

Perfect symmetry with respect to the bisecting plane of the dihedral corner is observed in the distribution of the longitudinal velocity component. It can be assumed that such symmetry also prevails for the transverse velocity component. This means that two vortices rotating in the opposite directions are formed in the zone of interaction between the boundary layers on both sides of the bisecting plane. Therefore, the distortion in the isotach distribution observed in Fig. 5b is directly related to the development of these vortices. Consequently, qualitative information on the direction and intensity of the transverse flow can be obtained with respect to the shape of the isotachs.

Let us analyze the behavior of flow characteristics in the interaction region as the Reynolds number Re_x and the pressure gradient $d\bar{p}/dx$ vary. Experiments on the effect of the Reynolds number were performed in the range of unperturbed flow velocities from 10 to 52 m/sec. Figure 5a, b shows only some of the results. Analysis of all the available data suggests that, in the investigated range of Re_x numbers, the direction of transverse flow remains constant, i.e., the pattern shown in Fig. 5b persists. For smaller Re_x numbers, the vortex spreads, as it were, to a larger area of the transverse cross section and also along the corner side. With an increase in Re_x, the vortex contracts, while its rotation axis shifts toward the line of intersection between the surfaces.

The above-mentioned variations in the scale and position of the vortex in the transverse section of the corner also influence considerably the extent of the interaction zone, the relative magnitude of which is shown in Fig. 6 for $d\bar{p}/dx = 0$. This figure also provides the experimental data for corners of channels with a square cross section [4–7]. The value of h is defined as the distance for which the isotach $u/u_\delta = 0.99$ deviates from the direction parallel to the wall. The vertical lines denote the errors in determining this value of h/δ_2 dimin-

ishes with an increase in Re_x in a rather wide range of Reynolds numbers, which vary by more than one order of magnitude. On the average, the extent of the interaction zone h amounts to approximately three boundary-layer thicknesses outside the interaction zone.

Figure 5b, c also shows the distributions of the equal-velocity curves for different longitudinal static pressure gradients. These and other data indicate that the characteristic distortion of isotachs in the interaction zone increases considerably with an increase in the pressure gradient. This is connected with the increasing role of the secondary flow, which is more intensive for positive than for negative pressure gradients. For this reason, the isotachs are distorted slightly for negative pressure gradients (left-hand part of Fig. 5c). The longitudinal pressure gradient exerts a considerable influence on the integral characteristics of the boundary layer, both inside and outside the interaction zone. For instance, the displacement thickness and the momentum loss thickness increase by a factor of approximately 2 with an increase in $d\bar{p}/dx$ under our conditions. Outside the interaction zone, the boundary-layer characteristics, including the local friction coefficient, are in satisfactory agreement with the numerical values obtained by means of the method described in [2]. The maximum deviation of the experimental values of c_f determined by means of the expression used in [8] from the theoretical values does not excees 3%.

The relative extent of the interaction zone h/δ_2 as a function of the longitudinal pressure gradient for $Re_x \simeq 1.72 \cdot 10^6$ is shown in Fig. 7. The vertical lines on the diagram denote the error in determining this quantity. The extent of the interaction zone increases with $d\bar{p}/dx$, while a positive pressure gradient exerts a greater influence. This can be explained by the more intensive development of secondary flow. The values of h/δ_2, obtained with a dummy wall and by varying the angle of attack of the simulator (solid and open circles, respectively), are approximated by means of a single relationship, $h/\delta_2 = f(d\bar{p}/dx)$.

The authors are grateful to V. M. Shulemovich and V. N. Dolgov, who performed the numerical calculations according to a special program, and to N. F. Polyakov for the useful discussions during preparation for the experiments.

LITERATURE CITED

1. G. I. Bagaev, A. A. Kurdin, N. F. Polyakov, and V. V. Chernykh, "Investigation of certain flow characteristics in a low-turbulence subsonic aerodynamic tunnel," in: Aero- and Gasdynamics [in Russian], Izd. ITPM Sibirsk. Otd. Akad. Nauk SSSR, Novosibirsk (1973).
2. V. N. Dolgov and V.M. Shulemovich, "Finite-difference calculation of an incompressible turbulent boundary layer with complex boundary conditions," in: Physical Gasdynamics [in Russian], Izd. ITPM Sibirsk. Otd. Akad. Nauk SSSR, Novosibirsk (1977).
3. O. O. Mojola and A. D. Young, "An experimental investigation of the turbulent boundary layer along a streamwise corner," AGARD-CP-93 (1971).
4. M. A. Paradis, "Couche limite turbulente á l'interieur d'un diedre," Labor. d'Aerodyn., Laval, Quebec, Canada (1963).
5. F. B. Gessner, "The origin of secondary flow in turbulent flow along a corner," J. Fluid, Mech., 58, 1 (1973).
6. H. J. Perkins, "The formation of streamwise vorticity in turbulent flow," J. Fluid Mech., 44, 4 (1970).
7. G. M. Bragg, "The turbulent boundary layer in a corner," J. Fluid. Mech., 36, 3 (1969).
8. H. Ludwieg and W. Tillman, "Investigation of the wall-shearing stress in turbulent boundary layers," NASA Tech. Mem. No. 1285 (1950).